



Effects of reconsolidation on cyclic deformation behaviours of a kaolin clay

Zhixuan Liang^{1,2} · Mingyue Kong¹ · Ying Liu^{1,3} · Maosong Huang² · Jian Gong¹

Received: 30 December 2023 / Accepted: 6 September 2024

© The Author(s), under exclusive licence to Springer-Verlag GmbH Germany, part of Springer Nature 2024

Abstract

Subgrades may be subjected to intermittent cyclic loads such as traffic loads. Under these loading conditions, excess pore water pressure can accumulate in clayey soils during cyclic loading period and dissipate during resting time. The deformation behaviour of clayey soil after reconsolidation process may be different from that under consecutive cyclic loading. A series of undrained cyclic triaxial tests, including reconsolidation process between cyclic loading stages, were performed on kaolin clay. The axial strain accumulation, excess pore water pressure accumulation, deviatoric stress–strain loop and resilience modulus under different cyclic stress ratios, initial confining pressures and degrees of reconsolidation were discussed and presented. Test results show that the reconsolidation process has significant effects on the deformation characteristics of clayey soil. The coupling effects of change of void ratio and effective mean stress result in a non-monotonic relationship between normalised total axial strain and degree of reconsolidation. In addition, an increase in the degree of reconsolidation leads to an increase in the normalised excess pore water pressure increment during 2nd cyclic loading stage, regardless of cyclic stress ratio and initial confining pressure. Furthermore, the steady resilience modulus at the end of each cyclic loading stage depends on the effective cyclic stress ratio and initial confining pressure, irrespective of reconsolidation process.

Keywords Axial strain accumulation · Cyclic triaxial tests · Degree of reconsolidation · Excess pore water pressure accumulation · Intermittent cyclic loading · Resilience modulus

1 Introduction

For cities located in estuary deltas, many transportation infrastructure were constructed on sedimentary soft clay, such as high-speed railway, highway, airport and subway [39]. These infrastructures are inevitably subjected to long-time traffic loadings during their service period, which is ultimately spread to subsoil [2, 5, 15, 17, 44, 48]. Under these cyclic loadings, strain and excess pore water pressure (EPWP) can accumulate in soils, resulting in a series of

engineering problems [15, 26, 29]. Traffic loading is always applied to subsoil discontinuously. Due to the low permeability of clayey soils, EPWP in soils may accumulate during cyclic loading period and dissipate in resting period under discontinuous traffic loadings [18, 25, 26]. After reconsolidation process in resting period, the subsoil became denser, and its mechanical characteristics may have changed. Thus, understanding the cyclic behaviours of clayey soils subjected to discontinuous traffic loading is critical to assess the performance of the existing structure in soft clay.

Many studies have been conducted to investigate the deformation behaviour of soil under consecutive cyclic loading. It is broadly recognised that the dynamic properties of soil are influenced by many factors, such as effective confining pressure, cyclic stress ratio (CSR), initial deviatoric stress ratio and loading frequency [6, 18, 28, 29, 38]. Qian et al. [29] performed a series of undrained cyclic heart-shaped tests on Shanghai clay using a hollow cylinder apparatus. The authors claimed that the undrained

✉ Ying Liu
lyily1112@126.com

¹ School of Civil Engineering and Architecture, Guangxi University, Nanning, Guangxi, China

² Department of Geotechnical Engineering, Tongji University, Shanghai, China

³ State Key Laboratory of Featured Metal Materials and Life-Cycle Safety for Composite Structures, Nanning, Guangxi, China

response of clay subjected to different stress levels can be described by the shakedown approach, including plastic shakedown, cyclic plastic creep and ratcheting (incremental instability). Qian et al. [28] conducted a series of undrained cyclic triaxial tests on over-consolidated Shanghai silty clay. These researchers observed that increasing the over-consolidation ratio (OCR) can result in a decrease in permanent and resilient strains, and the effect of OCR is remarkable for lightly over-consolidated samples. Guo et al. [6] investigated the undrained deformation behaviour of Wenzhou undisturbed soft clay subjected to long-term cyclic loading (50,000 loading cycles). The results indicated that with increase in confining pressure and CSR, the resilience modulus decreases more remarkably with increase in loading cycles. In addition, the authors established two equations to predict the long-term permanent strain and resilience modulus.

Most existing studies on the deformation behaviour of soft clay under traffic loading are based on partially drained or undrained consecutive cyclic tests [6, 14, 18, 19, 28, 29, 31]. However, consecutive cyclic loading patterns cannot properly reflect traffic loading. Partial or full cyclic loading-induced EPWP in subsoil can dissipate during nonoperational hours [18, 40, 41].

Considering the intermittent effect of traffic loading, some research based on multiple-stage cyclic loading tests where the drainage period is interspersed between loading cycles has been conducted [4, 13, 18, 25, 33, 46]. Yang and Cui [41] investigated the effect of intermittent traffic loads on saturated silty clay by cyclic triaxial tests. In their work, the samples were subjected to multiple-stage undrained cyclic loading, and 10 min was interspersed between loading cycles to allow drainage. An empirical prediction formula was established to describe the permanent strain of soil under such loading conditions. The effect of loading frequency on the deformation behaviour of Tianjin soft clay under 5-min interval cyclic loading was investigated by Lei et al. [13]. The authors discovered that intermittency strengthens the resistance of clay to degradation of shear modulus. A similar phenomenon was also reported by Zheng et al. [46], who conducted undrained triaxial tests on undisturbed marine sedimentary clay subjected to periodic intermittent cyclic loading. The effect of water content on cyclic deformation characteristics was investigated by Tong et al. [33] using hollow cylinder apparatus. To investigate the effect of resting period durations on the cyclic behaviour of clay, Liu and Xue [18] carried out both consecutive and intermittent cyclic loading on kaolin clay. These researchers observed that a decrease in the duration of the resting period can enlarge the overall accumulated axial strain of samples.

The above-mentioned studies regarding the intermittent effect of traffic loading are based on the duration of resting

time. Liu and Xue [18] claimed that, however, under those reconsolidation approaches, the distribution of EPWP in sample is nonuniform, and the property degree of reconsolidation (U_r) is difficult to obtain, which brings uncertainties to the evolution of stress and strain in the sample.

Feng et al. [4] analysed the reconsolidation behaviour of Wenzhou soft clays under intermittent cyclic loading, in which the quiescent period is long enough to fully dissipate EPWP. The experimental results show that the reconsolidation process leads to the non-deformability of marine sedimentary clays. Similar conclusions were reported by Yildirim and Ersan [45] and O'Reilly et al. [25]. Karakan et al. [11] investigated liquefaction and post-liquefaction settlement of a nonplastic silt and established relationships among factor of safety to liquefaction, post-liquefaction volumetric strain and relative density. These investigations are significant to clarify the effect of full reconsolidation on the cyclic behaviours of soils. However, due to the low permeability of clay, the transient reconsolidation time and the complex seepage path in subsoil, the property condition in foundation soil after cyclic loading is between full reconsolidation and no reconsolidation [8, 35]. Wang et al. [35] conducted a series of undrained cyclic and post-cyclic triaxial tests on marine reconstituted silty clay to investigate the effect of U_r on the post-cyclic monotonic characteristics of soil. In their work, after being subjected to undrained cyclic loading, the samples were allowed to drain to a specific back pressure to achieve desired U_r . Based on the test results, a post-cyclic strength model considering different U_r was established. Similar work was carried out by Huang et al. [7, 8] on laterite clay. However, among existing studies, the effect of different U_r on the cyclic behaviours of clayey soils is not clear and needs to be further investigated.

Based on review of exiting studies regarding the effect of intermittent traffic loading, it is found that there is limited study on the intermittent cyclic deformation behaviours of clayey soils based on uniform samples with residual EPWP and certain stress state. In this study, a series of cyclic triaxial tests were carried out on kaolin clay. In the tests, to simulate residual EPWP, as recommended by Huang et al. [7, 8] and Wang et al. [35], undrained cyclic loading was applied to the samples, and a reconsolidation process was allowed between two cyclic loading stages by controlling the specific back pressure. The effects of different U_r on the cyclic behaviour of clayey soil were studied. Furthermore, the influence of the confining pressure and CSR under different U_r on the cyclic deformation behaviour of soil was analysed and discussed.

2 Sample preparation and test programme

2.1 Sample preparation

An advanced dynamic triaxial testing system at Guangxi University was used to perform the cyclic triaxial tests. The system was manufactured by GDS Instruments Ltd., UK. More details of the system can be found in the work of Qian et al. [28].

The tested material in this study was a kaolin clay, which was widely used in geotechnical research to investigate mechanical characteristics of clayey soils [16, 18, 19, 24, 37]. The specific gravity of the clay is 2.6. The plastic limit and liquid limit are approximately 35% and 75%, respectively, with a plastic index of approximately 40%. More details regarding the clay can be found in the work of Nie et al. [24].

Slurry consolidation method was firstly proposed by Sheeran and Krizek [32] and be widely used in unit tests of reconstituted clay [15, 18, 19, 24, 37]. According to Wichtmann et al. [37] and Lin and Peaumedu [16] by measuring the water content at different location within kaolin specimen, the pre-consolidated sample prepared by slurry consolidation method was found quite homogeneous. In addition, slurry consolidation method can easily reach saturation and simulate well the soil fabric found within a hydraulic fill deposit [34]. To investigate the sedimentary clay under traffic facilities, the slurry consolidation was adopted in the study.

As suggested by Liu et al. [19] and Liang et al. [15], de-air water was mixed with clay powder to prepare slurries with a water content of approximately 150% (two times the liquid limit). The slurry was placed into a perspex tube mould with a size of 50 mm (inner diameter) \times 160 mm (height), and was pre-consolidated under a vertical pressure of 100 kPa. More details about the sample preparation process can be found in Liu et al. [19].

After pre-consolidation process, the samples were trimmed to a height of 60 mm with a diameter of 50 mm ($h/d = 1.2$). As claimed by Wichtmann et al. [36], the h/d ratio has limited effects on the cyclic behaviour of clayey soil under undrained triaxial dynamic loading. This dimension of sample was also used in Nie et al. [24] and is similar to that utilised in Ren et al. [30] and Liu et al. [19]. To saturate the sample, a back pressure of 400 kPa with an effective confining pressure of 20 kPa was applied. A Skempton's B value of at least 0.96 in all samples was achieved.

2.2 Test programme

Before applying cyclic loading, the stress state of real soil should be simulated. K_0 consolidation state is most realistic simulation method to the field, but requires high instruments, complicated test steps and relatively high cost [22, 23]. Compared to coarse grained materials, K_0 value of clayey soil is closer to 1. Thus, for simplifying the test operation, referring the existing research [7, 18, 23, 24, 28, 29, 33, 35], the simplified isotropic consolidation method is adopted in the study.

After being saturated, the samples were isotropically consolidated under an effective confining pressure of p'_o (100, 200, 400 kPa). The consolidation duration was kept at approximately 8 h to ensure full dissipation of EPWP of all samples. The axial strain rate of samples at the end of consolidation period is less than 0.018% per hour, which means that all the samples have completed primary consolidation [15, 19].

After isotropic consolidation, the first 10,000 one-way sinusoidal loading cycles with a frequency of 1 Hz were applied to all samples under undrained conditions. Considering the main purposes of this study, number of cycles and loading frequency were not considered as a research variable. Thus, to achieve stable EPWP of soils, 10,000 cycles were performed in each loading stage. As reported in previous studies [9, 10, 21], deformation behaviour of clay under undrained cyclic loading is essentially time-based creep phenomenon, and effect of frequency (lower than 10 Hz) on strain accumulation can be ignored. Thus, to simulate traffic load, the frequency of 1 Hz recommended by Qian et al. [29] is adopted in the study, which is in the range from 0.2 to 3 Hz recommended by Yang et al. [43]. The axial strain and EPWP of the samples would accumulate to ε_{ac}^{1cls} and Δu^{1cls} at the end of this loading phase, as expressed in Fig. 1a, b and c.

Then, the drainage valve was opened and the cyclic loading-induced EPWP (Δu^{1cls}) was allowed to dissipate to the applied back pressure (p_u) to achieve a certain U_r . The reconsolidation duration was maintained at approximately 8 h which is same to the consolidation period, to assure the dissipation is complete and the residual EPWP is evenly distributed in the soil sample. Following the research of Wang et al. [35] and Huang et al. [8], the degree of reconsolidation U_r is defined as the ratio of the dissipation of EPWP ($\Delta u'$) to the cyclic loading-induced EPWP (Δu^{1cls}) and can be expressed as:

$$U_r = \frac{\Delta u'}{\Delta u^{1cls}} = 1 - \frac{p_u}{\Delta u^{1cls}} \quad (1)$$

By controlling the applied back pressure, five different U_r (0, 25, 50, 75, 100%) were employed in this study. $U_r = 0\%$ represents that the samples were not

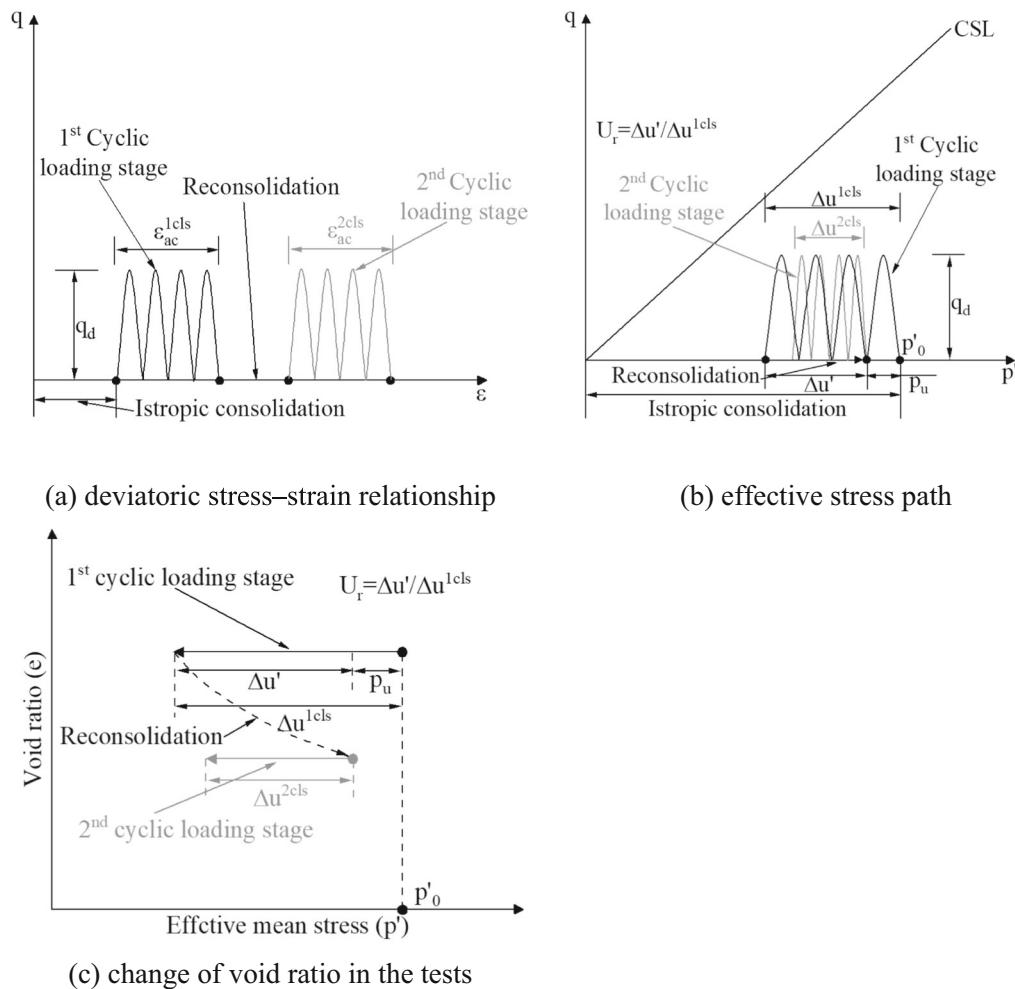


Fig. 1 Diagram of cyclic loading patterns used in the tests

reconsolidated, which means continuous loading with 20,000 cycles was applied on the samples.

After the reconsolidation process, the second 10,000 sinusoidal loading cycles were applied to the samples under undrained conditions. Same to the first 10,000 loading cycles, a frequency of 1 Hz was adopted. The axial strain and EPWP of the samples would accumulate with ε_{ac}^{2cls} and Δu^{2cls} at the end of this loading phase, as expressed in Fig. 1a, b and c.

The stress–strain relationship, effective stress path curves and change in void ratio from the tests are shown in Fig. 1a, b and c, respectively. The effective mean stress $p' = (\sigma_1 + 2\sigma_3)/3$ and the deviatoric stress $q = \sigma_1 - \sigma_3$ are applied, where σ_1 and σ_3 are the major and minor principal stress in the triaxial test. In this study, to systematically investigate the effects of reconsolidation on the cyclic behaviours of clayey soil, five different U_r and three different effective confining pressures p'_0 (100, 200, 400 kPa) under a cyclic stress ratio (CSR) of 0.2 were employed. In addition, a series of cyclic triaxial tests with

different CSR (0.1, 0.15, 0.2) and five different U_r were carried out on samples with an effective confining pressure of 200 kPa. The cyclic test schemes are summarised in Table 1.

3 Results and analysis

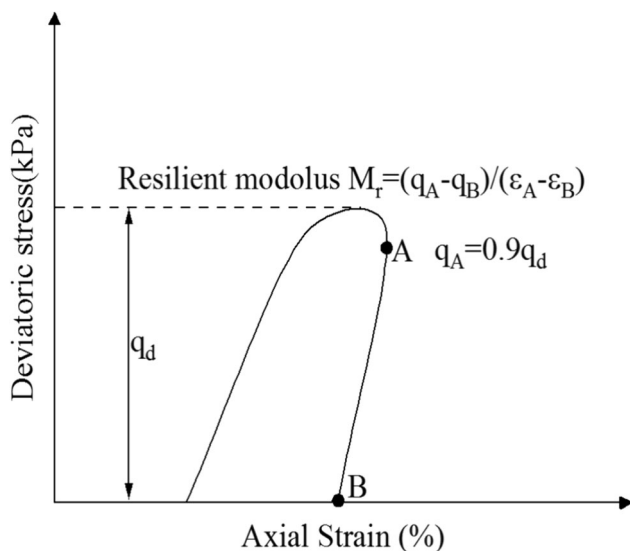
This section presents the effects of different U_r on the axial strain accumulation, EPWP accumulation and resilience modulus of tested samples. To ensure the consistency of data, as recommended by Alam et al. [1], the resilience modulus (M_r) can be calculated as follows:

$$M_r = \frac{q_A - q_B}{\varepsilon_A - \varepsilon_B} \quad (2)$$

where q_A and q_B refer to approximately 90% of the maximum deviatoric stress and minimum deviatoric stress in an unloading cycle, respectively. ε_A and ε_B correspond to the axial strain at q_A and q_B in an unloading cycle, respectively, as shown in Fig. 2.

Table 1 Undrained cyclic triaxial test series

Test series	Test id	p'_o (kPa)	q_d (kPa)	U_r (%)	CSR = q_d/p'_o	
1	p100q20u0	100	20	0	0.2	
	p100q20u25			25		
	p100q20u50			50		
	p100q20u75			75		
	p100q20u100			100		
	p200q40u0	200	40	0		
	p200q40u25			25		
	p200q40u50			50		
	p200q40u75			75		
	p200q40u100			100		
	p400q80u0	400	80	0		
	p400q80u25			25		
	p400q80u50			50		
	p400q80u75			75		
	p400q80u100			100		
2	p200q20u0	200	20	0	0.1	
	p200q20u25			25		
	p200q20u50			50		
	p200q20u75			75		
	p200q20u100			100		
	p200q30u0	30	0	0		0.15
	p200q30u25			25		
	p200q30u50			50		
	p200q30u75			75		
	p200q30u100			100		

**Fig. 2** The definition of the resilience modulus M_r , after Alam et al. [1]

3.1 The cyclic behaviour of soil during the 1st cyclic loading stage

Figure 3 shows the typical cyclic response of samples in 1st cyclic loading stage, which is obtained from the sample p200q40u100. As shown in Fig. 3a, with an increase in number of cycles, the axial strain accumulated significantly at the beginning and then tended to a steady and very slow growth. For example, the plastic axial strain increased from 0% to 0.37% in the first 1000 loading cycles, while it increased by 0.02% between loading cycles No. 9000 and 10,000. The accumulated EPWP shows similar developing trend, which would increase to a stable value with small oscillations, as shown in Fig. 3b. Figure 3c depicts the stress–strain loops of the sample and highlights a certain number of cycles. With increase in number of cycles, the stress–strain loops became inclined and thinner, and the stress–strain hysteresis loops change from unclosed to closed. Figure 3d shows the variation in the resilience modulus versus the number of cycles. It is clearly exhibited that the resilience modulus decreases rapidly in the early few cycles and then keeps basically stable at a certain value. Under cyclic loading with small amplitude, soil particles rearrange may be the reason for rapid increase of axial strain and EPWP in the initial loading phase. As the cyclic loading goes on, the soil is in a state of dynamic equilibrium. In a loading–unloading cycle, thin and closed stress–strain loops signify that the soil stain is recoverable and the material damping of soil became smaller. However, the decrease of resilience modulus indicates that soil skeleton is more fragile to deformation. Similar experimental phenomena have been reported by Qian et al. [27] and Liu et al. [19].

Figures 4 and 5 show the accumulated axial strain and EPWP at the end of 1st cyclic loading versus CSR or effective confining pressure. Figure 6 shows the resilience modulus and normalised resilience modulus at the end of 1st cyclic loading stage versus effective cyclic stress ratio (q_d/p'), in which p' corresponds to the effective mean stress at the end of 1st cyclic loading stage. Several parallel tests in the 1st cyclic loading stage were applied at the same CSR and effective confining pressure as the next stage required different degrees of reconsolidation. The test results are summarised in Table 2. Similar results in Figs. 4, 5, 6 and Table 2 prove the validity and repeatability of parallel tests. In other words, the sample difference caused by the sample preparation process can be ignored to some extent. As shown in Fig. 4, at the same confining pressure ($p'_o = 200$ kPa), the accumulated axial strain and EPWP increase exponentially with increase in CSR, which is in accordance with the work of Guo et al. [6]. As shown in Fig. 5, for the same CSR of 0.2, the accumulated axial

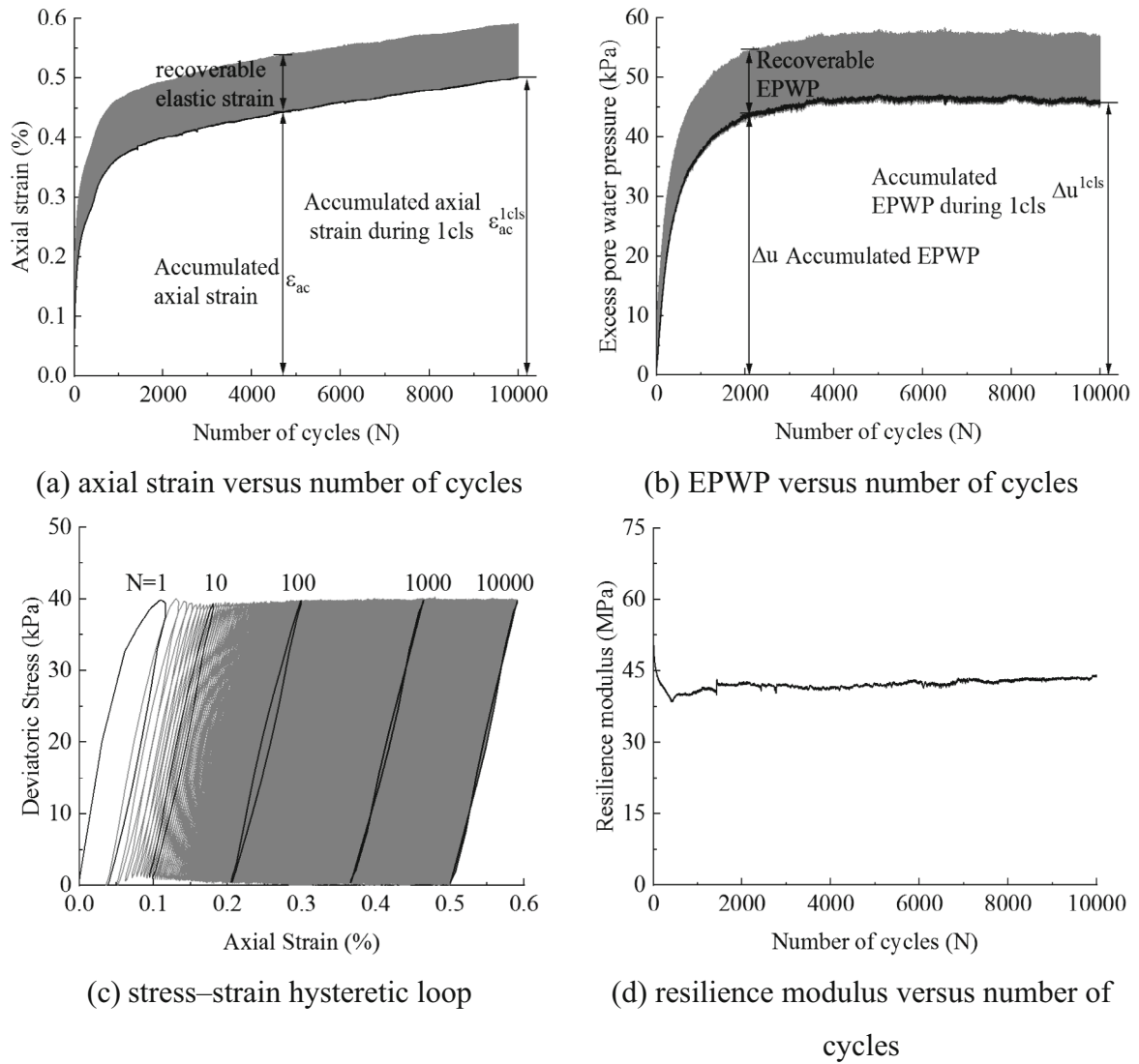


Fig. 3 Typical deformation behaviour of kaolin clay under undrained cyclic loading, (obtained from the sample p200q40u100)

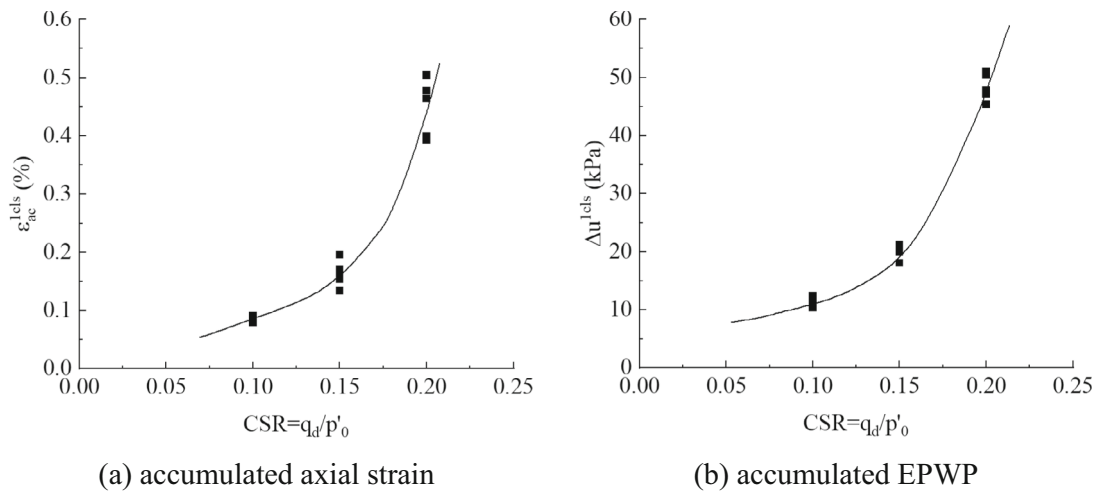


Fig. 4 Accumulated axial strain and EPWP during 10,000 cycles versus CSR (all samples were subjected to a p'_o of 200 kPa)

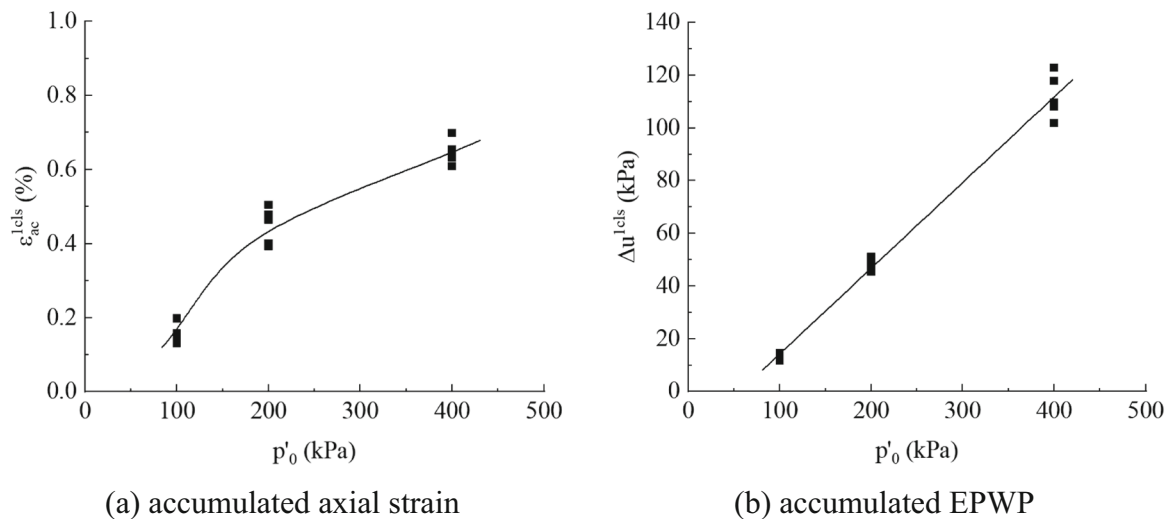


Fig. 5 Accumulated axial strain and EPWP during 10,000 cycles versus p'_0 (all samples were subjected to a CSR of 0.2)

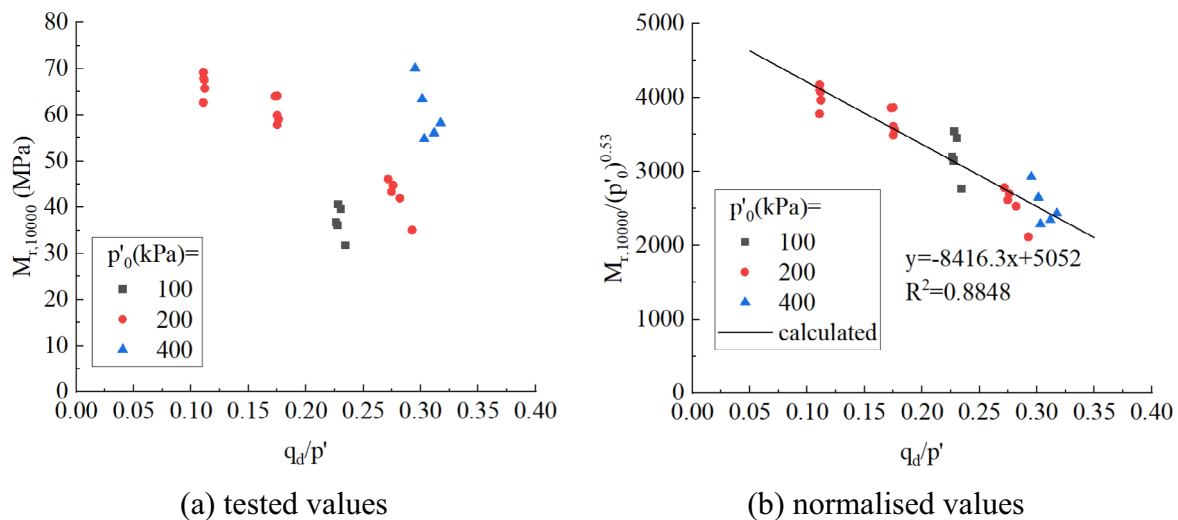


Fig. 6 Resilience modulus at No.10000 cycle versus effective CSR for different confining pressures

strain increases disproportionately with increase in confining pressure, while the EPWP increases linearly. The reason for such a phenomenon might be that a larger cyclic stress was applied to samples with greater p'_0 , as the CSR is constant at 0.2 [3, 18].

There is no obvious functional relationship between the steady resilience modulus at the end of the 1st cyclic loading stage and the effective CSR (q_d/p'), as shown in Fig. 6a. Then, the steady resilience modulus was normalised by the k power of initial confining pressure (p'_0), where the exponent k (in this study, $k = 0.53$) is a fitting parameter, which reflects the nonlinear relationship between initial confining pressure (p'_0) and resilience modulus, as illustrated in Fig. 6b. The nonlinear relationship has also been reported in previous works [20, 47]. As can be seen in the figure, the resilience modulus under

different initial confining pressures falls together into a single curve and decreases with increase in q_d/p' . Similar results have been reported by Liu et al. [19] and Guo et al. [6].

3.2 The cyclic behaviour of soil after the reconsolidation process

As suggested by Liu and Xue [18], to investigate the effects of reconsolidation on the cyclic deformation behaviour of soils, the axial strain produced by the reconsolidation process was excluded from the accumulated axial strain in this section.

Table 2 The results of undrained cyclic triaxial test

Test id	1st cyclic loading stage			2nd cyclic loading stage			$\varepsilon_{ac}^{2cls}/\varepsilon_{ac}^{1cls}$	$\Delta u^{2cls}/\Delta u^{1cls}$
	ε_{ac}^{1cls} (%)	Δu^{1cls} (kPa)	$M_{r,10000}$ (MPa)	ε_{ac}^{2cls} (%)	Δu^{2cls} (kPa)	$M_{r,20000}$ (MPa)		
p100q20u0	0.144	13.3	39.6	0.042	- 0.5	39.4	0.29	- 0.04
p100q20u25	0.130	12.4	40.6	0.059	1.8	42.6	0.45	0.15
p100q20u50	0.198	14.7	31.8	0.082	3.9	36.7	0.41	0.27
p100q20u75	0.158	11.7	36.7	0.076	3.4	40.8	0.48	0.29
p100q20u100	0.153	12.1	36.1	0.085	5.9	40.4	0.56	0.49
p200q40u0	0.478	50.5	35.1	0.077	- 0.5	34.8	0.16	- 0.01
p200q40u25	0.400	47.1	43.4	0.131	6.6	40.4	0.33	0.14
p200q40u50	0.464	47.9	44.8	0.103	14.0	45.1	0.22	0.29
p200q40u75	0.393	51.0	42.0	0.178	17.3	43.3	0.45	0.34
p200q40u100	0.505	45.4	46.1	0.288	16.8	48.0	0.57	0.37
p400q80u0	0.609	101.8	70.1	0.100	- 2.3	71.8	0.16	- 0.02
p400q80u25	0.632	108.0	63.4	0.174	17.3	63.9	0.28	0.16
p400q80u50	0.655	117.8	56.1	0.151	31.7	63.5	0.23	0.27
p400q80u75	0.699	122.8	58.3	0.212	39.5	67.0	0.30	0.32
p400q80u100	0.646	109.7	54.8	0.297	42.0	74.7	0.46	0.38
p200q20u0	0.086	12.4	65.7	0.032	- 0.6	66.3	0.38	- 0.04
p200q20u25	0.087	11.8	67.6	0.049	2.1	69.1	0.56	0.18
p200q20u50	0.092	10.6	67.9	0.045	3.1	70.4	0.50	0.29
p200q20u75	0.083	10.5	69.2	0.048	4.6	68.7	0.58	0.44
p200q20u100	0.080	10.4	62.7	0.069	3.8	61.1	0.86	0.37
p200q30u0	0.196	21.2	59.1	0.048	0.6	60.1	0.25	0.03
p200q30u25	0.171	19.9	57.8	0.080	2.4	59.2	0.46	0.12
p200q30u50	0.160	20.0	64.1	0.071	4.7	76.0	0.45	0.23
p200q30u75	0.154	20.0	59.9	0.086	8.4	65.4	0.56	0.42
p200q30u100	0.134	18.1	64.0	0.127	8.7	62.1	0.95	0.48

3.2.1 Variation in accumulated axial strain

Figure 7 illustrates the axial strain accumulation during the two cyclic loading stage of all samples. In the figures, the accumulated axial strain (ε_{ac}) was normalised by the accumulated axial strain during the 1st cyclic loading stage (ε_{ac}^{1cls}). As seen, compared with those under consecutive cyclic loading ($U_r = 0\%$), greater cyclic axial strain accumulation was observed in samples including reconsolidation process. For instance, the total normalised accumulated axial strain with samples subjected to $p'_o = 200$ kPa and $q_d = 40$ kPa after two cyclic loading stages are approximately 1.34, 1.22, 1.45 and 1.57 under the U_r of 25, 50, 75 and 100%, respectively, while it is approximately 1.16 under consecutive cyclic loading ($U_r = 0\%$). Liu et al. [18, 19] claimed that after a number of consecutive cyclic loading cycles, the soil reaches a relatively stable state, resulting in continuous and steady axial strain accumulation. Reconsolidation process may disturb the stable state of the soil. Thus, during subsequent cyclic loading, a new balance needs to be established for soil

particles, resulting in greater strain accumulation in soil [18].

To eliminate the influence of initial confining and cyclic stress ratio on the strain accumulation behaviour of soil, as illustrated in Fig. 8, the accumulated axial strain during the 2nd cyclic loading stage (ε_{ac}^{2cls}) was normalised by the accumulated axial strain during the 1st cyclic loading stage (ε_{ac}^{1cls}). It can be clearly seen in Fig. 8 that greater axial strain accumulates in samples including reconsolidation process than in those under consecutive cyclic loading ($U_r = 0\%$). In addition, it is worth noting that the $\varepsilon_{ac}^{2cls}/\varepsilon_{ac}^{1cls}$ values are less than 1 for all samples, which indicates that less strain accumulated in soil during the 2nd cyclic loading stage. According to Xia et al. [40] and Yildirim and Ersan [45], the reason for less strain accumulation is the dissipation of EPWP and the reduction in the void ratio in soils induced by reconsolidation, which could strengthen the cyclic resistance of soil.

The effects of reconsolidation on axial strain accumulation under different initial confining pressures and CSR are illustrated in Fig. 8a, b, respectively. As discussed

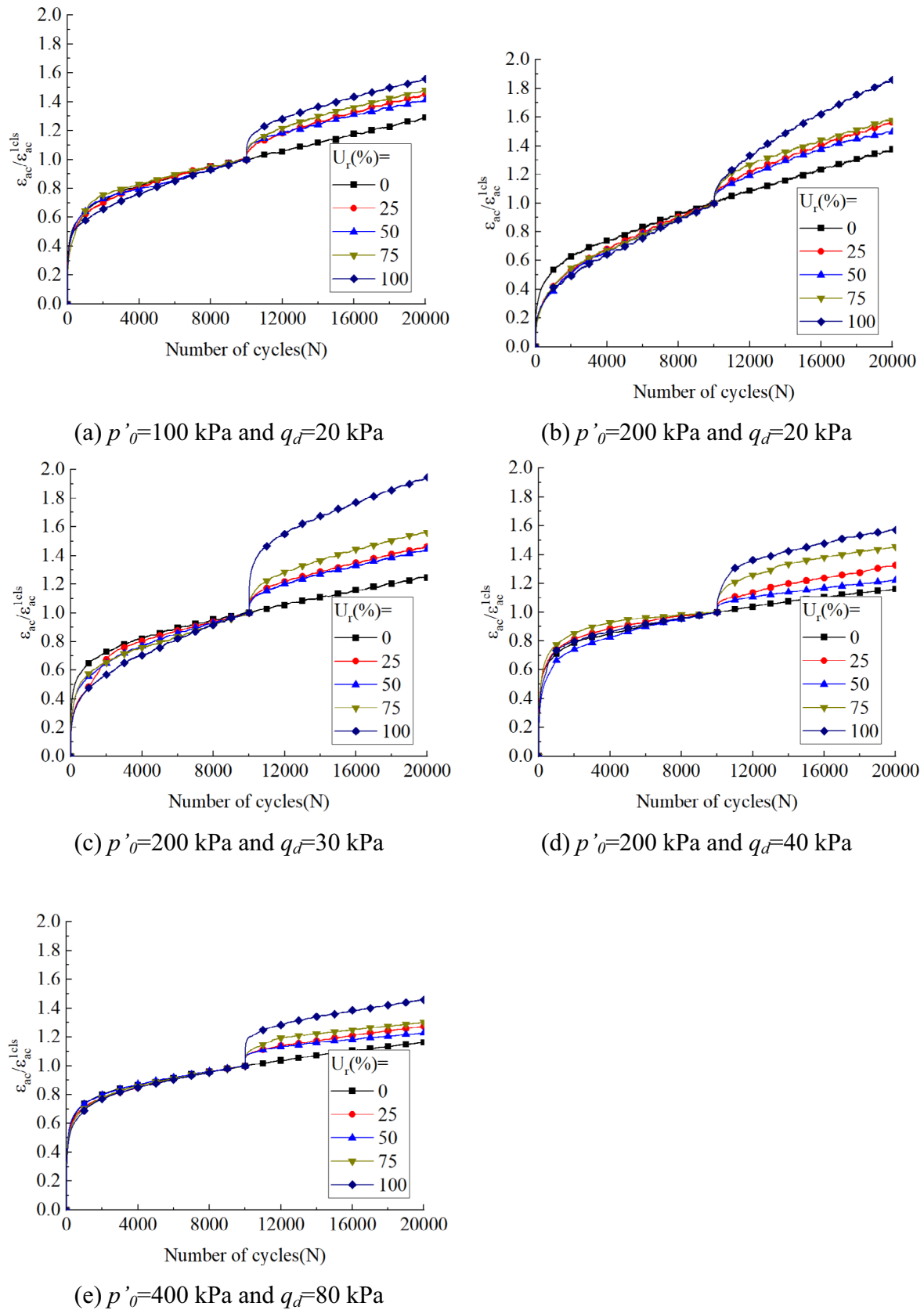


Fig. 7 Normalised axial strain accumulation versus the number of cycles

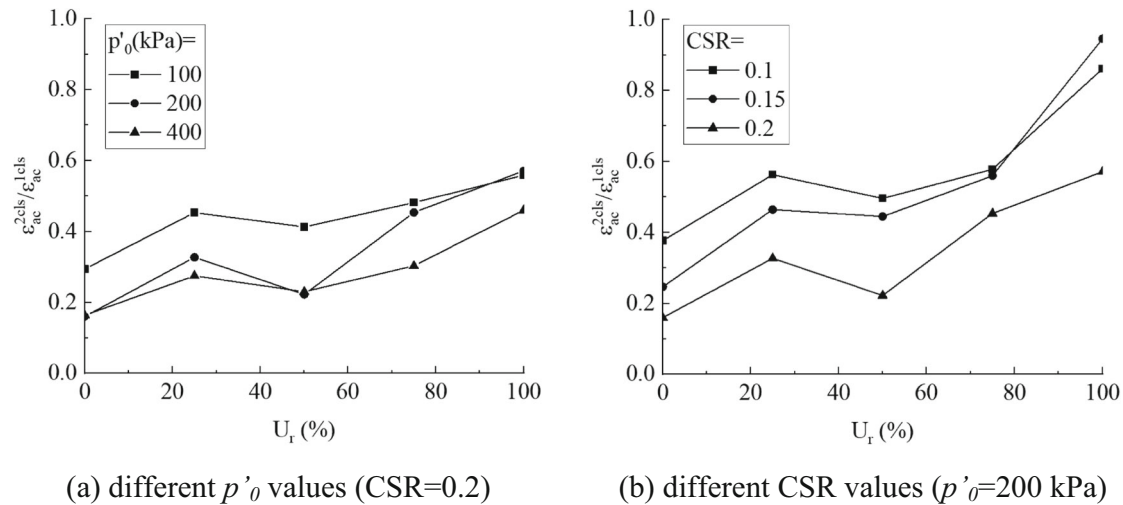


Fig. 8 Normalised axial strain increment during the 2nd cyclic loading stage versus U_r

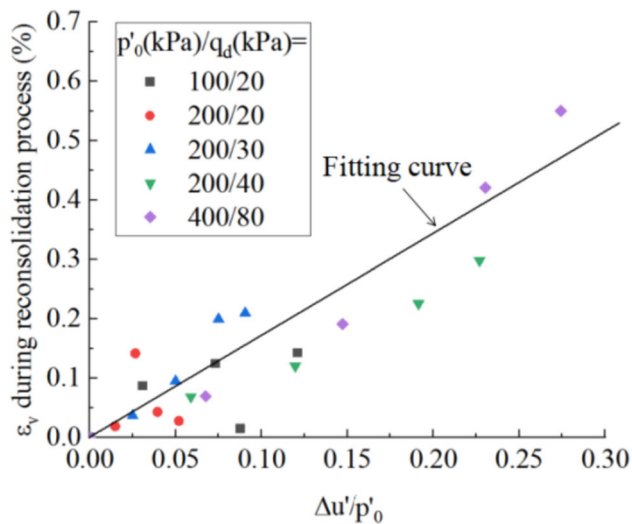


Fig. 9 Relationship between the volume strain and normalised dissipation of EPWP during reconsolidation process

earlier, less strain could accumulate in soil during the 2nd cyclic loading stage. Figure 8a, b reveals that the larger the initial confining pressure or CSR is, the smaller the $\varepsilon_{ac}^{2cls}/\varepsilon_{ac}^{1cls}$ values. This is because a larger p'_0 or CSR value corresponds to a larger accumulated EPWP, as illustrated in Figs. 4b and 5b, which leads to a greater volumetric strain during reconsolidation process, as illustrated in Fig. 9. Thus, a sample subjected to a larger p'_0 or CSR value becomes denser, resulting in a greater decrease in axial strain during the 2nd cyclic loading stage. A similar effect of change of void ratio on the strain accumulation behaviour of soil was reported by Liu et al. [19]. Noting that the $\varepsilon_{ac}^{2cls}/\varepsilon_{ac}^{1cls}$ value of sample p200q30u100 is 0.95, which is higher than that of sample p200q20u100. The possible reason for this might attribute to experimental errors. As can be seen in Table 2, ε_{ac}^{1cls} value of sample

p200q30u100 is 0.134%, which is the lowest in the group (samples subjected to $p'_0 = 200$ kPa and $q_d = 30$ kPa), resulting in a higher $\varepsilon_{ac}^{2cls}/\varepsilon_{ac}^{1cls}$ value, and this deviation may be induced by the discrepancy in sample preparation, temperature change and instrument operation.

As shown in Fig. 8, an increase in U_r will lead to an increase in the $\varepsilon_{ac}^{2cls}/\varepsilon_{ac}^{1cls}$ value as a whole. Interestingly, the $\varepsilon_{ac}^{2cls}/\varepsilon_{ac}^{1cls}$ ratio does not increase monotonically with increase in U_r , and it decreases as U_r increases from 25 to 50%. Such a phenomenon occurred in all tested samples, irrespective of p'_0 and CSR, which has not been reported in previous studies. The reason for this finding might be attributed to the coupling effects of change of void ratio and the effective mean stress. On the one hand, under the same p'_0 and CSR conditions, an increase in U_r will lead to a greater change of void ratio and a greater change of soil particle arrangement, resulting in violently breaking the cyclic balance established in the 1st cyclic loading stage, which will induce greater ε_{ac}^{2cls} . On the other hand, an increase in U_r refers to more dissipation of accumulated EPWP and an increase in the mean effective stress, so the particles are arranged more closely which is beneficial for cyclic resistance. For the samples under consecutive cyclic loading ($U_r = 0\%$), although the effective mean stress at the beginning of the 2nd cyclic loading stage is the lowest compared with those including reconsolidation process, the axial strain accumulates at a slowest rate because the homeostasis established in the 1st cyclic loading stage was not disturbed. For the samples with $U_r = 25\%$, 75% and 100% , the void ratio change plays a leading role in the 2nd cyclic loading, and the $\varepsilon_{ac}^{2cls}/\varepsilon_{ac}^{1cls}$ values continue to increase. For the samples with $U_r = 50\%$, the $\varepsilon_{ac}^{2cls}/\varepsilon_{ac}^{1cls}$ are lower than those samples with $U_r = 25\%$, which means the mean effective stress has prevailed on this occasion. When considering the effect of reconsolidation on

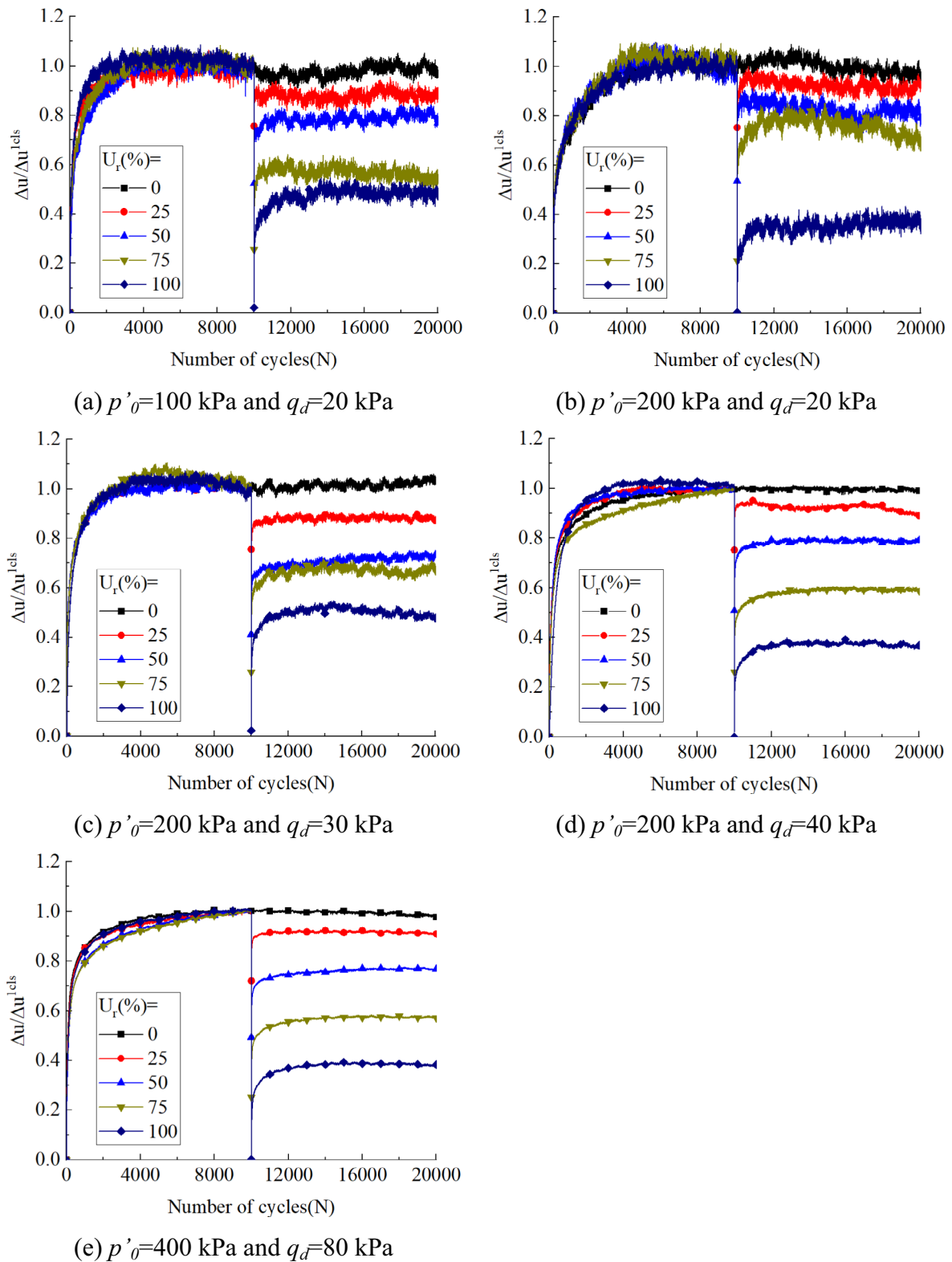


Fig. 10 Normalised EPWP accumulation versus number of cycles

settlement of foundation soil in practical engineering, it should not only pay attention to the favourable side of

denser soil particle arrangement, but also pay more attention to the unfavourable side of broken cyclic balance.

3.2.2 Variation in the accumulated EPWP

Figure 10 illustrates the EPWP accumulation of all samples. In the figures, the accumulated EPWP (Δu) was normalised by the accumulated EPWP during the 1st cyclic loading stage ($\Delta u^{1\text{cls}}$). After the reconsolidation process, partial or all EPWP was dissipated in soils, resulting in the $\Delta u/\Delta u^{1\text{cls}}$ values of samples of $U_r = 25, 50, 75$ and 100% “jump” to 0.75, 0.5, 0.25 and 0 at the beginning of the 2nd cyclic loading stage, respectively. Compared with those under consecutive cyclic loading ($U_r = 0\%$), the EPWP accumulated significantly in the sample including reconsolidation process. Clearly, as shown in Fig. 10, including reconsolidation process can reduce the EPWP in samples during 2nd cyclic loading stage, and the greater the U_r value is, the lower the $\Delta u/\Delta u^{1\text{cls}}$ values at the end of the 2nd cyclic loading. For instance, the $\Delta u/\Delta u^{1\text{cls}}$ values with samples subjected to $p'_{o} = 200$ kPa and $q_d = 40$ kPa after two cyclic loading stages are approximately 0.89, 0.79, 0.59 and 0.37 under the U_r values of 25, 50, 75 and 100% , respectively, while they are approximately 0.98 under consecutive cyclic loading ($U_r = 0\%$). Such findings might be attributed to the smaller void ratio of samples with higher U_r . Under the same p'_{o} and CSR conditions, an increase in U_r will lead to a greater change of volume strain, as illustrated in Fig. 9, resulting in a lower void ratio of samples. The EPWP at the end of the 2nd cyclic loading stage decreased due to the lower void ratio Yildirim and Ersan [45].

To eliminate the influence of initial confining and cyclic stress ratio on the EPWP accumulation behaviour of soil, as illustrated in Fig. 11, the accumulated EPWP during the 2nd cyclic loading stage ($\Delta u^{2\text{cls}}$) was normalised by the accumulated EPWP during the 1st cyclic loading stage

($\Delta u^{1\text{cls}}$). Interestingly, the $\Delta u^{2\text{cls}}/\Delta u^{1\text{cls}}$ values increase with increase in U_r , regardless of initial confining pressure p'_{o} and CSR. The larger the U_r value is, the greater the change in the void ratio, which leads to a more thorough break in the cyclic equilibrium, resulting in a greater normalised EPWP in the 2nd cyclic loading stage. Notably, increasing U_r will also lead to an increase in the effective mean stress, resulting in an increase in cyclic resistance of the sample. In addition, the $\Delta u^{2\text{cls}}/\Delta u^{1\text{cls}}$ values show a monotonic increasing relationship with U_r . This means that, compared with increase in effective stress, the change of void ratio plays a predominant role in pore pressure accumulation behaviour during 2nd cyclic loading stage.

Notable is, the $\Delta u^{2\text{cls}}/\Delta u^{1\text{cls}}$ values of samples (subjected to $p'_{o} = 200$ kPa and CSR = 0.1) decrease as U_r values increase from 75 to 100% . Under a relative low CSR condition, EPWP accumulates little. As can be seen in Table 2, $\Delta u^{1\text{cls}}$ values of samples (subjected to $p'_{o} = 200$ kPa and CSR = 0.1) are in the range from 10.4 to 12.4 kPa and $\Delta u^{2\text{cls}}$ values of these sample are less than 6 kPa. In this case, the fluctuation of pore pressure due to temperature change or other reasons has significant effect on the value of $\Delta u^{2\text{cls}}/\Delta u^{1\text{cls}}$, and this may be the reason for this abnormal downward trend. Despite these experimental errors, it can still be concluded that the $\Delta u^{2\text{cls}}/\Delta u^{1\text{cls}}$ values monotonically increase along with U_r values.

3.2.3 Variation in the resilience modulus

To investigate the effects of reconsolidation process on the resilience modulus of soil, Fig. 12a, b shows the typical deviatoric stress–strain loop and normalised resilience modulus versus the number of cycles, respectively. In the figures, the samples were subjected to a confining pressure

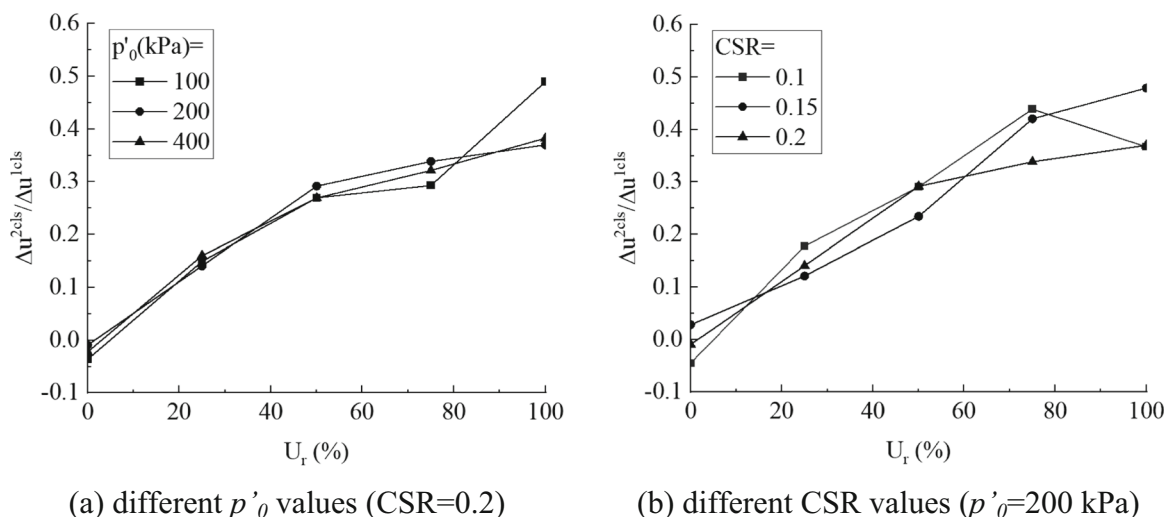
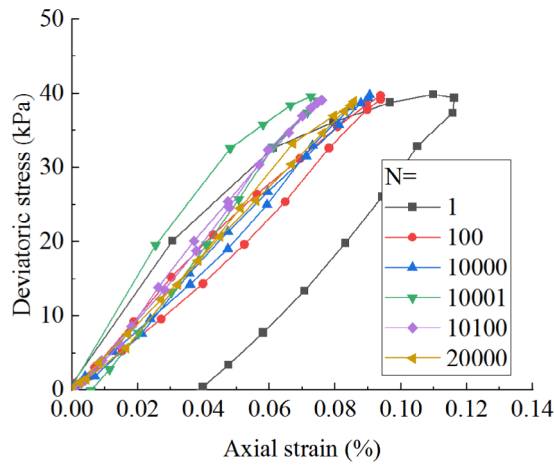
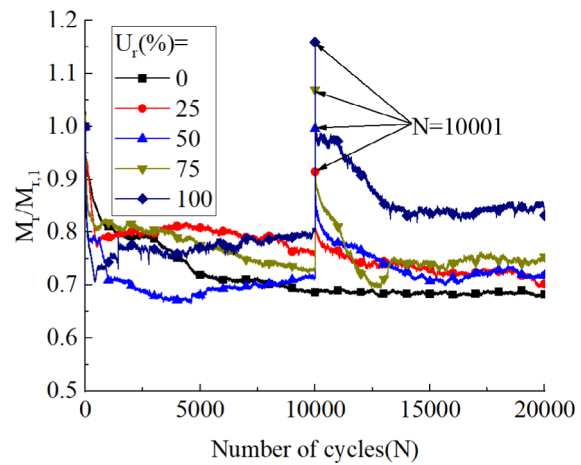


Fig. 11 Normalised EPWP increment during the 2nd cyclic loading stage versus degree of reconsolidation



(a) deviatoric stress–strain hysteretic loop ($U_r=100\%$)



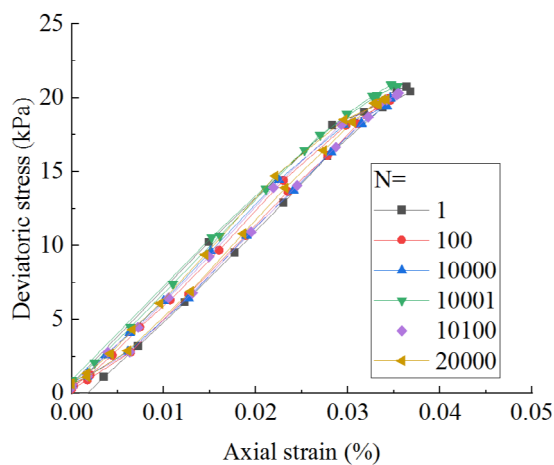
(b) normalised resilience modulus versus number of cycles

Fig. 12 Typical stress–strain loop and normalised resilience modulus versus number of cycles ($p'_o = 200$ kPa, $q_d = 40$ kPa)

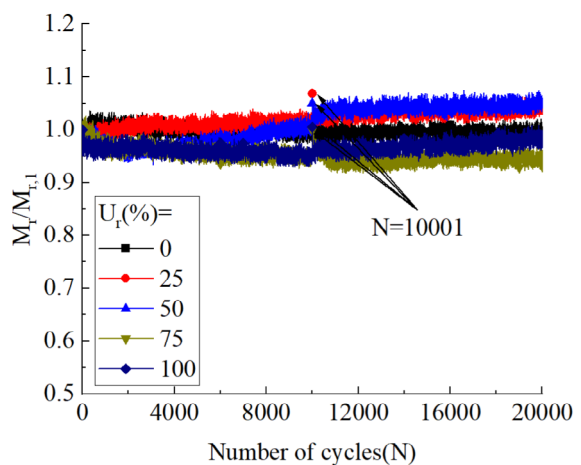
of 200 kPa and a CSR of 0.2. To compare the stress–strain response at different numbers of cycles, the typical stress–strain loops (Nos. 1, 100, 10,000, 10,001, 10,100, 20,000) of the sample with $U_r = 100\%$ are plotted in Fig. 12a, in which the accumulated strain was subtracted from total strain. During the 1st cyclic loading stage, as mentioned above, the stress–strain loops became thinner and the stress–strain hysteresis loops change from unclosed to closed. However, after the reconsolidation process, the stress–strain loop of No. 10001 cycle reopened and became steep, which implies axial strain reaccumulation and stiffness hardening. The increase in stiffness might be attributed to the increase in effective mean stress and decrease of

void ratio [4, 18]. As cyclic loading continued in 2nd loading stage, the stress–strain loops became thinner again and the stress–strain hysteresis loops change to be closed, and the new dynamic elastic equilibrium has been formed. The stress–strain loop inclined to the horizontal axis, indicating cyclic stiffness degradation also occurred during the 2nd cyclic loading stage, which can be explained by the accumulation of the EPWP, as illustrated in Fig. 10d.

The stiffness hardening behaviour after the reconsolidation process can be observed in Fig. 12b, in which the resilience modulus M_r was normalised by the resilience modulus of the first cycle $M_{r,1}$. Figure 12b shows that an increase in U_r will result in an increase in the $M_r/M_{r,1}$ value



(a) deviatoric stress–strain hysteretic loop ($U_r=100\%$)



(b) normalised resilience modulus versus number of cycles

Fig. 13 Typical stress–strain loop and normalised resilience modulus versus number of cycles ($p'_o = 200$ kPa, $q_d = 20$ kPa)

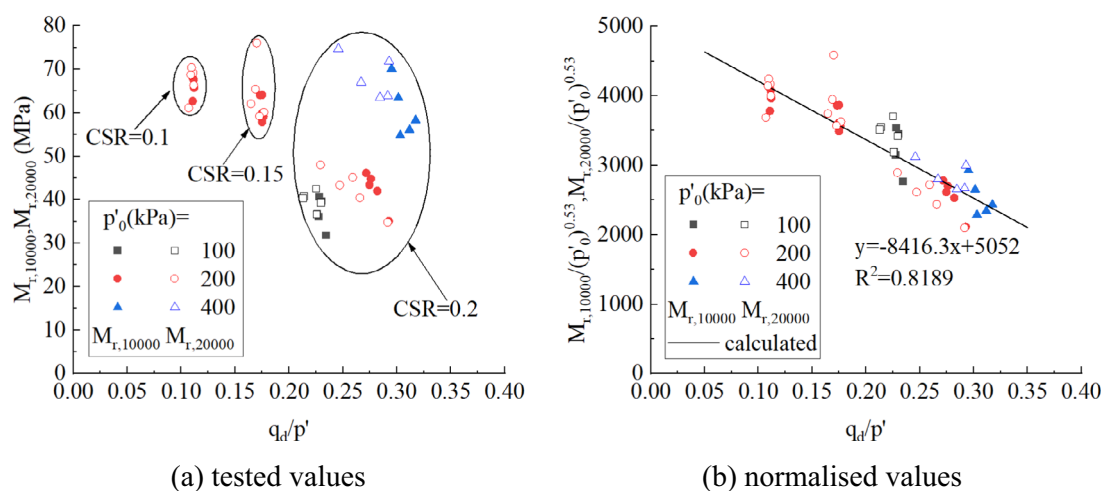


Fig. 14 Resilience modulus at No. 10000 and 20,000 cycles versus effective CSR for different confining pressures

at No.10001 cycle, indicating greater stiffness hardening behaviour due to the reconsolidation process. Under the same p'_0 and CSR conditions, an increase in U_r can lead to a decrease of void ratio and an increase in the effective mean stress, which are both beneficial for cyclic resistance [4, 18]. As cyclic loading continued, the resilience modulus decreased and reached a steady value at the end of the 2nd cyclic loading stage. However, for the samples under a relatively low cyclic stress ratio (CSR = 0.1), the resilience modulus seems to be little affected by the reconsolidation process, regardless of the degree of reconsolidation, as illustrated in Fig. 13.

The resilience modulus at the end of 1st cyclic loading stage ($M_{r,10000}$) and 2nd cyclic loading stage ($M_{r,20000}$) versus q_d/p' are plotted in Fig. 14a, in which p' is the mean effective stress at the end of corresponding cyclic loading stage, and the solid points represent $M_{r,10000}$ and the hollow points represent $M_{r,20000}$. For the samples of CSR = 0.2, both $M_{r,10000}$ and $M_{r,20000}$ will be bigger as the confining pressure is higher. Compared with $M_{r,10000}$, data points of $M_{r,20000}$ move up to the upper left, indicating that the resilience modulus has increased to some extent. For the samples of CSR = 0.1, however, the hollow points are very close to the solid points. This is because a lower CSR leads to smaller EPWP accumulation during the 1st cyclic loading stage, as illustrated in Fig. 4b, resulting in fewer effective mean stress increments and void ratio changes. Thus, the resilience modulus was minimally affected by the reconsolidation process. The increase in p'_0 has a similar effect to the increase in CSR on EPWP accumulation during the 1st cyclic loading stage, as illustrated in Fig. 5b, which results in a similar effect of q_d/p' value on the resilience modulus, as illustrated in Fig. 14a.

The $M_{r,10000}$ and $M_{r,20000}$ values normalised by the k power of initial confining pressure p'_0 versus q_d/p' are

shown in Fig. 14b. As discussed early, symbol k reflects the nonlinear relationship between initial confining pressure and resilience modulus and in this study, $k = 0.53$. The normalised M_r data fall together into a single curve, which is obtained from optimal fitting of $M_{r,10000}$, as illustrated in Fig. 6b. It can be concluded that the steady resilience modulus at the end of cyclic loading depends on the initial confining pressure p'_0 and q_d/p' value, regardless of the reconsolidation process.

According to Zhou et al. [47] and Qian et al. [28], under the same loading conditions, the sample with a smaller void ratio (a higher OCR) corresponds to a closer particle arrangement, which brings a smaller elastic strain and higher resilient modulus in cyclic loading. In this study, after reconsolidation process, tested specimens became denser due to the dissipation of cyclic loading-induced EPWP, as illustrated in Fig. 1c. However, the hollow point ($M_{r,20000}$) does not deviate from the optimal fitting curve of the solid point ($M_{r,10000}$), as illustrated in Fig. 14b. This means that compared to q_d/p' and p'_0 , the change of void ratio has limited effect on resilience modulus of tested samples. A possible reason for this phenomenon might attributed to the smaller void ratio changes in reconsolidation process compared to over-consolidation process and it needs to be further investigated.

4 Discussions

Figure 15 shows the first stress–strain loops of 2nd cyclic loading stage after different degrees of reconsolidation under the same $p'_0 = 200$ kPa, in which $U_r/N = 0/10001$ represents the stress–strain loop of $N = 10,001$ under continuously cyclic loading, and $U_r/N = 25/10001$ represents the first stress–strain loop after a reconsolidation of

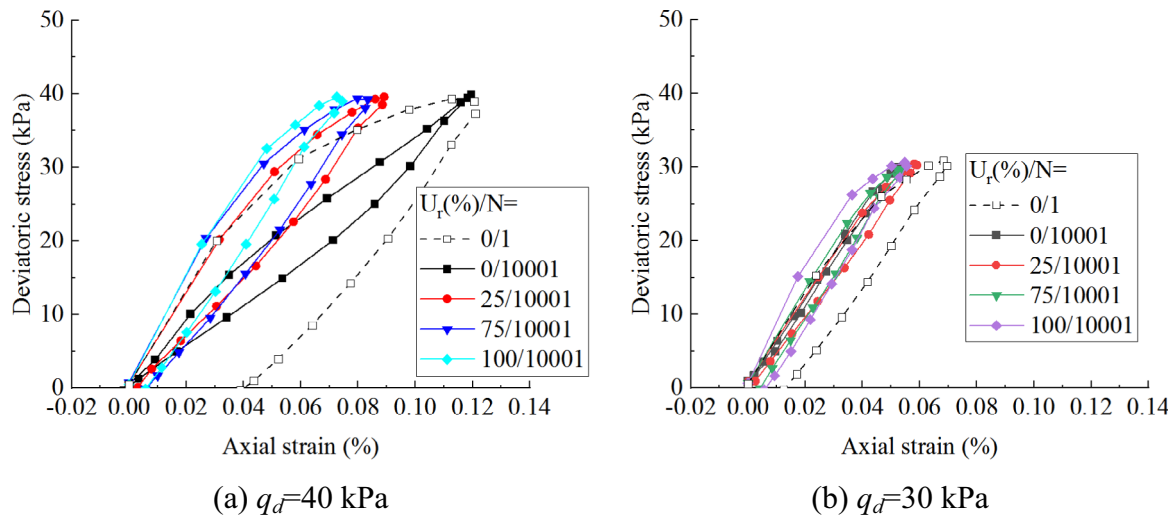


Fig. 15 The tress–strain loops for different reconsolidation degrees ($p'_o = 200$ kPa)

25% excess pore water pressure dissipated. The initial stress–strain loop is also displayed in Fig. 15 a in the form of dotted line for comparison. It can be seen from the shape evolution process of stress–strain loops, during the 1st cyclic loading stage, as mentioned above, the stress–strain loops change from fatter and unclosed to thinner and closed, which indicates the soil change from elastoplastic to dynamic elastic. Moreover, obvious stiffness weakening is found under larger dynamic stress ($q_d = 40$ kPa). The reconsolidation process breaks the dynamic equilibrium. The higher the U_r value, the more intensely breaking the dynamic elastic equilibrium. As reflected in Fig. 15a, b, in which stress–strain loops became fatter and unclosed again after reconsolidation, and the higher the U_r value, the more skewed to the vertical axis. Steeper initial loading curves signify the soil rearranged more closely after reconsolidation. The shape evolution process of stress–strain loops reveals again that the effect of reconsolidation on 2nd cyclic loading is reflected in two aspects. On the one hand, reconsolidation violently break the cyclic balance established in the 1st cyclic loading, which will induce greater ε_{ac}^{2cls} and Δu^{2cls} in the 2nd cyclic loading. On the other hand, an increase in U_r refers to an increase in the mean effective stress, so the particles are arranged more closely, which might be the reason for the obvious growth of resilience modulus M_r and excess pore pressure in the initial stage of 2nd cyclic loading.

5 Conclusions

To investigate the effects of reconsolidation on the undrained cyclic behaviours of clayey soils, a series of undrained cyclic triaxial tests including reconsolidation

processes between loading cycles were performed on kaolin clay. The variation in axial strain accumulation, excess pore water pressure accumulation, stress–strain characteristics and resilience modulus of samples under different degrees of reconsolidation, effective confining pressures and cyclic stress ratios were discussed and presented. Based on the limited number of cyclic triaxial tests, the conclusions are summarised as follows:

1. The normalised axial strain of samples after the reconsolidation process was significantly accumulated. An increase in the initial confining pressure or cyclic stress ratio could lead to a decrease in the normalised total axial strain. The coupling effects of the change of void ratio and effective mean stress result in a non-monotonic relationship between the degree of reconsolidation and normalised total axial strain. The settlement of foundation soil in practical engineering might be underestimated if ignoring the influence of reconsolidation.
2. The normalised excess pore water pressure increment during the 2nd cyclic loading stage depends on the degree of reconsolidation, and the larger the degree of reconsolidation is, the greater the values, regardless of the cyclic stress ratio and initial confining pressure.
3. The steady M_r values at the end of cyclic loading depend on the initial confining pressure and q_d/p' values, regardless of the reconsolidation process.

Supplementary Information The online version contains supplementary material available at <https://doi.org/10.1007/s11440-024-02399-5>.

Acknowledgements The project was funded by the National Natural Science Foundation of China (No.52278337, No.51968005), the Guangxi Natural Science Foundation (No. 2019GXNSFBA185038)

and Guangxi Science and Technology Major Project (No. AA23073018).

Author contributions Zhixuan Liang was involved in conceptualization, methodology, investigation, validation, formal analysis, visualisation, writing—review and editing. Mingyue Kong helped in data curation, investigation, writing—original draft. Ying Liu helped in funding acquisition, writing—review and editing. Maosong Huang contributed to writing—review and editing. Jian Gong contributed to writing—review and editing. All authors reviewed the manuscript.

Data availability Some or all data, models or code that supports the findings of this study is available from the corresponding author upon reasonable request.

Declarations

Conflict of interest The authors declare no competing interests.

References

- Alam MJJ, Gnanendran CT, Lo SR (2017) Modelling the settlement behavior of a strip footing on sloping sandy fill under cyclic loading conditions. *Comp Geotech* 86:181–192
- Chai JC, Miura N (2002) Traffic-load-induced permanent deformation of road on soft subsoil. *J Geotech Geoenviron Eng* 128(11):907–916
- Chen C, Zhou ZM, Kong LW, Zhang XW, Yin S (2018) Undrained dynamic behavior of peaty organic soil under long-term cyclic loading, Part I: experimental investigation. *Soil Dynam Earthq Eng* 107:279–291
- Feng D, Zhu X, Wang J, Cai Y, Guo L, Du Y (2020) The effects of cyclic loading on the reconsolidation behaviors of marine sedimentary clays under intermittent drainage conditions. *Soil Dynam Earthq Eng* 140:106510
- Ge SP, Yao XJ, Ye B, Pu ST, Liu XZ (2016) Analysis of long-term settlement of soft clay under train vibration. *Chin J Rock Mech Eng* 35(11):2359–2368
- Guo L, Wang J, Cai Y, Liu H, Gao Y, Sun H (2013) Undrained deformation behavior of saturated soft clay under long-term cyclic loading. *Soil Dyn Earthq Eng* 50:28–37
- Huang J, Chen J, Yu S (2023) Postcyclic stiffness behaviors of laterite clay under various conditions. *Int J GeoMech* 20(4):06023003
- Huang J, Chen J, Ke W, Zhong Y, Lu Y, Yi S (2021) Post-cyclic mechanical behaviors of laterite clay with different cyclic confining pressures and degrees of reconsolidation. *Soil Dyn Earthq Eng* 151:106986
- Hyde AFL, Brown SF (1976) The plastic deformation of a silty clay under creep and repeated loading. *Geotechnique* 26(1):173–184
- Hyde AFL, Yasuhara K, Hirao K (1993) Stability criteria for marine clay under one-way cyclic loading. *J Geotech Eng ASCE* 119(11):1771–1789
- Karakan E, Tanrini N, Sezer A (2019) Cyclic undrained behavior and post liquefaction settlement of a nonplastic silt. *Soil Dyn Earthq Eng* 120:214–227
- Kuerbis RH, Vaid YP (1988) Sand sample preparation—the slurry deposition method. *Soils Found* 28(4):107–118
- Lei H, Liu M, Feng S, Liu J, Jiang M (2020) Cyclic behavior of Tianjin soft clay under intermittent combined-frequency cyclic loading. *Int J GeoMech* 20(10):04020186
- Li D, Selig ET (1996) Cumulative plastic deformation for fine-grained subgrade soils. *J Geotech Engrg* 122:1006–1013
- Liang Z, Liu Y, Liu Z (2023) The undrained behavior of over-consolidated clay subjected to pure rotation of principal stress directions. *Mar Georesour Geotec* 41(9):1013–1025
- Lin H, Penumadu D (2005) Experimental investigation on principal stress rotation in Kaolin clay. *J Geotech Geoenviron* 131(5):633–642
- Liu Y, Liang Z, Liu Z, Nie G (2022) Post-cyclic drained shear behavior of Fujian sand under various loading conditions. *J Mar Sci Eng* 10(10):1499
- Liu Z, Xue J (2022) The deformation characteristics of a kaolin clay under intermittent cyclic loadings. *Soil Dyn Earthq En* 153:107112
- Liu ZY, Xue JF, Mei GX (2021) The impact of stress disturbance on undrained cyclic behavior of a kaolin clay and settlement of tunnels under cyclic loading. *Acta Geotech* 16(12):3947–3961
- Lu C, Chen JY, Gu C, Wang J, Cai YQ, Zhang TT, Lin G (2021) Resilient and permanent deformation behaviors of construction and demolition wastes in unbound pavement base and subbase applications. *Transp Geotech* 28:100541
- Matsui T, Ohara H, Ito T (1980) Cyclic stress-strain history and shear characteristics of clay. *J Geotech Engrg Div ASCE* 106(10):1101–1119
- Mayne PW (1985) Stress anisotropy effects on clay strength[J]. *J Geotech Eng* 111(3):356–366
- Meng XC, Liu R, Liang C (2024) Research on undrained shear strength properties of saturated clay. *J Civ Eng* 57(05):86–98
- Nie GP, Liu Y, Liu ZY, Liang ZX, Xue JF, Liang YW (2023) The Effects of drainage conditions on the cyclic deformation characteristics of over consolidated clayey soil. *Int J Civ Eng* 21(4):603–615
- O'reilly MP, Brown SF, Overy RF (1991) Cyclic loading of silty clay with drainage periods. *J Geotech Geoenviron* 117(2):354–362
- Price AB, DeJong JT, Boulanger RW (2017) Cyclic loading response of silt with multiple loading events. *J Geotech Geoenviron Eng* 143(10):04017080
- Qian JG, Du ZB, Yin ZY (2018) Cyclic degradation and non-coaxiality of soft clay subjected to pure rotation of principal stress directions. *Acta Geotech* 13(4):943–959
- Qian JG, Li SY, Zhang JL, Jiang JH, Wang QY (2019) Effects of OCR on monotonic and cyclic behavior of reconstituted Shanghai silty clay. *Soil Dyn Earthq Eng* 118:111–119
- Qian JG, Wang YG, Yin ZY, Huang MS (2016) Experimental identification of plastic shakedown behavior of saturated clay subjected to traffic loading with principal stress rotation. *Eng Geol* 214:29–42
- Ren XW, Xu Q, Teng JD, Zhao N, Lv L (2018) A novel model for the cumulative plastic strain of soft marine clay under long-term low cyclic loads. *Ocean Eng* 149:194–204
- Sakai A, Samang L, Miura N (2003) Partially-drained cyclic behavior and its application to the settlement of a low embankment road on silty-clay. *Soils Found* 43(1):33–46
- Sheeran DE, Krizek RJ (1971) Preparation of homogeneous soil samples by slurry consolidation. *J Mater* 6(2):356–373
- Tong L, Xue W, Ding H (2023) Influence of water content on clay deformation characteristics subjected to periodic intermittent loading. *Soil Dyn Earthq Eng* 171:107996. <https://doi.org/10.1016/j.soildyn.2023.107996>
- Wang S, Luna R, Stephenson RW (2011) A slurry consolidation approach to reconstitute low-plasticity silt specimens for laboratory triaxial testing. *Geotec Testing J* 34(4):288–296
- Wang Y, Lei J, Wang Y, Li S (2019) Post-cyclic shear behavior of reconstituted marine silty clay with different degrees of

- reconsolidation. *Soil Dyn Earthq Eng* 116:530–540. <https://doi.org/10.1016/j.soildyn.2018.10.042>
36. Wichtmann T, Andersen KH, Sjursen MA, Berre T (2013) Cyclic behavior of high-quality undisturbed block samples of Onsøy clay. *Can Geotech J* 50(4):400–412
 37. Wichtmann T, Triantafyllidis T (2018) Monotonic and cyclic tests on kaolin: a database for the development, calibration and verification of constitutive models for cohesive soils with focus to cyclic loading. *Acta Geotec* 13:1103–1128
 38. Wu HN, Shen SL, Chai JC, Zhang DM, Xu YS (2015) Evaluation of train-load-induced settlement in metro tunnels. *P I Civil Eng-Geotec* 168(5):396–406
 39. Wu T, Cai Y, Guo L (2017) Influence of shear stress level on deformation behaviour of undisturbed soft clay under traffic loading. *Eng Geol* 228
 40. Xia ZF, Ye GL, Wang JH, Ye B, Zhang F (2010) Fully coupled numerical analysis of repeated shake-consolidation process of earth embankment on liquefiable foundation. *Soil Dynam Earthq Eng* 30(11):1309–1318
 41. Yang JQ, Cui ZD (2020) Influences of train speed on permanent deformation of saturated soft soil under partial drainage conditions. *Soil Dynam Earthq Eng* 133:106120
 42. Yang Q, Tang YQ, Yuan B, Zhou J (2019) Cyclic stress-strain behavior of soft clay under traffic loading through hollow cylinder apparatus: effect of loading frequency. *Road Mater Pavem Des* 20:1026–1058
 43. Yang Q, Tang YQ, Yuan B, Zhou J (2019) Cyclic stress-strain behaviour of soft clay under traffic loading through hollow cylinder apparatus: effect of loading frequency. *Road Mater Pavem Des* 20:1026–1058
 44. Yasuhara K, Andersen KH (1991) Recompression of normally consolidated clay after cyclic loading. *Soils Found* 31(1):83–94
 45. Yildirim H, Ersan H (2007) Settlements under consecutive series of cyclic loading. *Soil Dynam Earthq Eng* 27(6):577–585
 46. Zheng Q, Xia T, Ding Z, He S (2019) The effect of periodic intermittency on the cyclic behavior of marine sedimentary clay. *Mar Georesour Geotechnol* 37(8):945–959
 47. Zhou ZW, Bai RQ, Shen MD, Wang QZ (2021) The effect of overconsolidation on monotonic and cyclic behaviours of frozen subgrade soil. *Transp Geotech* 32:100710
 48. Zou WL, Ding LQ, Han Z, Wang XQ (2020) Effects of freeze-thaw cycles on the moisture sensitivity of a compacted clay. *Eng Geol* 278(5):105832

Publisher's Note Springer Nature remains neutral with regard to jurisdictional claims in published maps and institutional affiliations.

Springer Nature or its licensor (e.g. a society or other partner) holds exclusive rights to this article under a publishing agreement with the author(s) or other rightsholder(s); author self-archiving of the accepted manuscript version of this article is solely governed by the terms of such publishing agreement and applicable law.